



Fibroblast-derived IL-33 is dispensable for lymph node homeostasis but critical for CD8 T cell responses to acute and chronic viral infection

Patricia Aparicio-Domingo<sup>1</sup>, H  l  ne Cannelle<sup>1</sup>, Matthew B. Buechler<sup>2</sup>, Sylvain Nguyen<sup>1</sup>, Sandra M. Kallert<sup>3</sup>, St  phanie Favre<sup>1</sup>, Nagham Alouche<sup>1</sup>, Natalie Papazian<sup>4</sup>, Burkhard Ludwig<sup>5</sup>, Tom Cupedo<sup>4</sup>, Daniel D. Pinschewer<sup>3</sup>, Shannon J. Turley<sup>2</sup>, Sanjiv A. Luther<sup>1</sup>

Keywords: Interleukin-33, alarmin, fibroblastic reticular cells, FRC, LCMV

<sup>1</sup> Department of Biochemistry, University of Lausanne, Epalinges, Switzerland

<sup>2</sup> Department of Cancer Immunology, Genentech, South San Francisco, United States

<sup>3</sup> Department of Biomedicine, Division of Experimental Virology, University of Basel, Basel, Switzerland

<sup>4</sup> Department of Hematology, Erasmus University Medical Center, Rotterdam, The Netherlands

<sup>5</sup> Institute of Immunobiology, Kantonsspital St.Gallen, St.Gallen, Switzerland

List of abbreviations used:

LN : Lymph Nodes

FRC: Fibroblastic Reticular Cell(s)

MedRC: Medullary Fibroblastic Reticular Cell(s)

Received: 19/09/2019; Revised: 02/06/2020; Accepted: 21/07/2020

This article has been accepted for publication and undergone full peer review but has not been through the copyediting, typesetting, pagination and proofreading process, which may lead to differences between this version and the [Version of Record](#). Please cite this article as [doi: 10.1002/eji.48413\\_FINAL](#).

This article is protected by copyright. All rights reserved.

TRC: T zone Fibroblastic Reticular Cell(s)

LEC: Lymphatic Endothelial Cell(s)

BEC: Blood Endothelial Cell(s)

HEV: High Endothelial Venules

LCMV: Lymphocytic Choriomeningitis Virus

DAMP : Damage-Associated Molecular Pattern(s)

Pdpr: Podoplanin

Correspondence:

Sanjiv Luther, Center for Immunity and Infection, Department of Biochemistry, University of Lausanne, Chemin des Boveresses 155, 1066 Epalinges, Switzerland;

Phone +41 21 692 5678; fax +41 21 692 5705; e-mail: sanjiv.luther@unil.ch

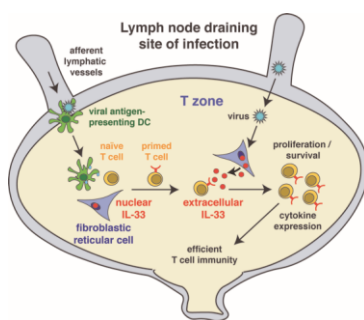
### **Abstract**

Upon viral infection, stressed or damaged cells can release alarmins like interleukin-33 (IL-33) that act as endogenous danger signals alerting innate and adaptive immune cells. IL-33 coming from non-hematopoietic cells has been identified as important factor triggering the expansion of anti-viral CD8<sup>+</sup> T cells. In lymph nodes (LN) the critical cellular source of IL-33 is unknown, as is its potential cell-intrinsic function as a chromatin-associated factor. Using IL-33-GFP reporter mice, we identify fibroblastic reticular cells (FRC) and lymphatic endothelial cells (LEC) as the main IL-33 source. In homeostasis, IL-33 is dispensable as a transcriptional regulator in FRC, indicating it functions mainly as released cytokine. Early during infection with lymphocytic choriomeningitis virus (LCMV) clone 13, both FRC and LEC lose IL-33 protein expression suggesting cytokine release, correlating timewise with IL-33 receptor expression by reactive CD8<sup>+</sup> T cells and their greatly augmented expansion in

wildtype versus  $Il33^{-/-}$  mice. Using mice lacking IL-33 selectively in FRC versus LEC we identify FRC as key IL-33 source driving acute and chronic anti-viral T cell responses. Collectively, these findings show that LN T zone FRC not only regulate the homeostasis of naïve T cells but also their expansion and differentiation several days into an antiviral response.

Graphical abstract blurb : less than 50 words

Interleukin-33 is an alarmin stored within nuclei of fibroblasts localizing to T zones of lymph nodes where naïve cytotoxic T cells get primed by viral-antigen presenting dendritic cells. This IL-33 gets released once the fibroblasts sense this viral infection leading to much more efficient T cell expansion and effector function.



## Introduction

Our immune system has evolved sophisticated strategies to defend our body against harmful infections produced by various pathogens. The critical first step is the detection of infection, which is typically followed by the activation of various immune cells and the elimination of the pathogen and infected cells. To sense microbial agents at early stages of infection, innate immune cells express receptors for pathogen-associated molecular patterns (PAMP) that lead to an inflammatory response. A second class of innate immune receptors recognize endogenous signals released during tissue damage, also known as damage-associated molecular patterns (DAMP), and these receptors are capable of alerting both innate and adaptive immune cells. Among the DAMP, the interleukin (IL)-1 family member IL-33 has emerged as central signaling molecule involved in multiple infections and pathologies [1-3]. It is prestored as a nuclear protein in epithelial cells of many mucosal body surfaces, as well

as in many endothelial cells, and it can be rapidly released as an alarm signal ('alarmin') from these cells upon infection, cellular stress, or necrosis. Various immune cells express the IL-33 receptor ST2, including granulocytes, innate lymphoid cells, regulatory T cells and activated T cells, with IL-33 recognition leading to their activation, expansion and/or differentiation [1-3].

While IL-33 has been extensively studied as a driver of Th2-driven allergic inflammation, recent evidence points to another role for IL-33 in driving primary CD8<sup>+</sup> T cell and CD4<sup>+</sup> Th1 responses within secondary lymphoid organs. IL-33- and ST2-deficient mice were shown to have a strongly reduced expansion of antigen-specific T cells in response to infection with various RNA and DNA viruses, suggesting a conserved IL-33-dependent mechanism for enhancing anti-viral immunity [4, 5]. Interestingly, radiation-resistant cells within the splenic T zone were identified as the relevant IL-33 source for anti-viral CD8<sup>+</sup> T cell responses [4] consistent with previous histological staining showing *Il33* transcription and IL-33 protein staining mainly in alpha-smooth muscle actin- and desmin-positive reticular cells of the T zone of murine spleen and murine and human lymph nodes (LN) [6, 7]. However, gene array analysis of sorted stromal cells from naive murine LN indicated additional complexity with podoplanin (Pdpn)<sup>+</sup> CD31<sup>-</sup> fibroblastic reticular cells (FRC) and Pdpn<sup>+</sup>CD31<sup>+</sup> lymphatic endothelial cells (LEC) being able to express *Il33* [8]. Therefore, it is possible that one or more distinct cell types function as key source of IL-33 that critically impacts anti-viral CD8<sup>+</sup> T cell responses in LN. Currently, we lack a good understanding of the IL-33-expressing LN stroma subsets, their precise localization and function during anti-viral immunity.

IL-33 is being called a dual function cytokine as it can act not only as an extracellular molecule on ST2 expressing cells but also can regulate gene transcription due to its nuclear localization and binding of DNA-associated histones [9, 10]. Previous studies on the cell intrinsic and ST2-independent role of IL-33 have focused on cell lines transfected with IL-33 siRNA which showed a downregulation of proinflammatory cytokine and protease expression in epithelial, endothelial, and fibroblastic cells, with CHIP assays suggesting the binding of IL-33 to the promoter sequences of IL-13 and NF-κB p65 [10-12]. Other studies suggested the opposite, namely the repression of transcription in epithelial cells [9, 13] which was not confirmed at the proteome level [14]. Yet another study described the overexpression of IL-

33 in an epithelial cell line with no transcriptional changes observed in a genome-wide analysis [15]. So far, only one recent study compared *ex vivo* cells, namely wildtype (wt) versus *Il33*<sup>-/-</sup> pro-B cells, and uncovered many transcriptional changes in absence of IL-33 with mixed bone marrow chimera experiments indicating these effects are cell-intrinsic [16]. Together, these data suggest that IL-33 can regulate gene transcription but that this property is cell-type and context-dependent. So far, no study has reported on the transcriptional role of IL-33 in LN stroma.

LN are complex structures composed of both stromal and hematopoietic cells that primarily function to retain pathogens or pathogen-carrying cells from lymph fluid and present them to naive or memory lymphocytes that recirculate via these structures, entering from blood vessels and leaving via lymphatic vessels. The inner core of secondary lymphoid tissues is organized by various FRC subsets that have been recognized as important players in lymphoid organ development, homeostasis and adaptive immunity [17-19]. FRC along with CD35<sup>+</sup> follicular dendritic cells constitutively express chemokines that segregate T cells, B cells and other immune cells into distinct compartments, such as the T zone, B zone and medulla. Follicular FRC and follicular dendritic cells express B cell chemokines to attract naive B cells [20], while medullary FRC (MedRC) selectively associate with plasma cells and innate immune cells [21]. T zone FRC (TRC) produce CCL19 and CCL21, which attract dendritic cells (DC) and naive T cells into that compartment [22, 23], thereby facilitating the selection and activation of rare antigen-specific T lymphocytes. It is within the T zone that these T cells expand and differentiate into effector cells before leaving the organ to home to peripheral sites of infection and inflammation.

In the current study, we performed a detailed characterization of the cellular sources of IL-33 in LN, both in homeostasis and during viral infection, and tested the role of these IL-33 sources in augmenting anti-viral T cell responses *in vivo*. We also investigated the importance of IL-33 in regulating gene expression in *ex vivo* isolated LN FRC using RNA sequencing. Our results show that FRC subsets throughout the T zone and medullary cords as well as LEC within the medulla are the main IL-33 sources in murine and human LN under homeostatic conditions, with no limiting role observed for gene regulation in murine fibroblasts of naive LN. Upon acute or chronic infection with two lymphocytic

choriomeningitis virus (LCMV) strains, stromal cells remained the major IL-33 source. To identify the critical stromal IL-33 source in LN, we generated and analyzed mice lacking IL-33 selectively in stromal cell subsets and identified IL-33 expression by FRC but not LEC as being critical for efficient anti-viral CD8<sup>+</sup> T cell responses, both during the acute and chronic phase of the response, demonstrating a novel role for FRC in complementing the functions of DC during the clonal expansion of anti-viral CD8 T effector cells.

## Results

### FRC and endothelial cells are the main producers of IL-33 in murine and human lymph nodes

Previous histological analysis of murine LN has indicated that IL-33<sup>+</sup> cells within T zones are  $\alpha$ SMA-expressing fibroblasts, [6, 7] partially contradicting gene array data of sorted stromal cells where both FRC and LEC were identified as major IL-33 sources [8]. To better characterize the IL-33 expressing cell types within naive murine LN [7], both by histology and flow cytometry, we made use of the *Il33*<sup>gfp/+</sup> mouse strain [24] where GFP is knocked into the translational start site of that locus to act as reporter of IL-33 promoter activity and transcription, while also abolishing detectable IL-33 protein expression from that allele [25]. In agreement with earlier findings in spleen [24], immunostainings of peripheral LN sections for GFP and IL-33 protein demonstrated that virtually all IL-33 transcribing cells also express IL-33 protein (Fig. 1A), with protein expression being lost in *Il33*<sup>gfp/gfp</sup> (= *Il33*<sup>-/-</sup>) mice (Supporting Information Fig. 1A), corroborating the faithfulness of this reporter strain also in LN. GFP expression was observed throughout the T zone and interfollicular region (IFR), while being absent in B cell follicles, again consistent with our histological staining for IL-33 protein (Fig. 1A) and with data reported for lacZ-reporter mice [7]. In addition, we noted a marked signal for *Il33* expression in medullary regions. To identify the cellular source, we initially performed histological co-staining for IL-33, GFP and cellular markers. Indeed, reticular Pdpn<sup>+</sup> FRC in the T zone and medullary cords made up most of the IL-33<sup>+</sup> cells, both for proteins and transcripts. We identified the additional IL-33<sup>+</sup> cells as Lyve1<sup>+</sup> lymphatic vessels, which were enriched within medullary sinuses (Fig. 1B). In both cell types, IL-33 protein localized to the nucleus (Supporting Information Fig 1B, data not shown), similar to

published data on epithelial and endothelial cells [6]. As expected, CD31<sup>+</sup> high endothelial venules (HEV) did not express IL-33 protein in murine LN [6, 7]. However, reticular cells surrounding these vessels and possibly representing pericytes often expressed IL-33 (Fig. 1B).

To characterize the IL-33 transcribing cells at the single cell level and in a quantitative manner, we performed flow cytometric analysis of CD45<sup>-</sup> stromal cells isolated enzymatically from naive LN of *Il33<sup>gfp/+</sup>* mice, using the combination of Pdpn and CD31 to identify FRC, LEC and blood endothelial cells (BEC) (Fig. 1C, Supporting Information Fig. 2A). A large fraction of all FRC were GFP<sup>+</sup> (~67%; Fig. 1D and E), comparable to our previous findings for naive spleen FRC [24]. Endothelial expression of IL-33 was less prominent with ~27% of LEC exhibiting a GFP signal. Further, BEC were almost all negative for GFP expression as were all hematopoietic cell subsets investigated (Fig. 1D-F), confirming our histological analysis. In absolute cell numbers, FRC were the predominant IL-33 source with many fewer LEC being positive (Fig. 1E). These data, which were based on GFP reporter expression, were confirmed by RT-PCR analysis of *Il33* transcripts in sorted cell subsets (Fig. 1G) and are in line with the previously published gene array data [8]. We observed abundant *Il33* transcripts and GFP in the two major FRC subsets, TRC and MedRC (Fig. 1G and Supporting Information Fig. 1C-D, 2A), yet *Il33* transcript levels measured in seven different cell types were highest in sorted TRC, which represent the FRC subtype colocalizing with naive T cells.

Also in human LN,  $\alpha$ SMA<sup>+</sup> and desmin<sup>+</sup> T zone fibroblasts have been proposed to be a major IL-33 source, in addition to HEV [6, 7, 26]. We observed abundant IL-33 protein expression in Pdpn<sup>+</sup> FRC of human LN, both inside the T zone and IFR, with B cell follicles lacking IL-33 protein expression (Fig. 1H and Supporting Information Fig. 1E). Lyve1<sup>+</sup> lymphatic vessels of the medulla and CD31<sup>+</sup> blood vessels with HEV-like morphology were also associated with strong IL-33 expression (Fig. 1H and Supporting Information Fig. 1E). In summary, the pattern of IL-33 distribution is fairly conserved in human and mouse LN including the expression by FRC in T zones and IFR, and by LEC in the medullary regions.

### **IL-33 is dispensable for FRC homeostasis and signature gene expression**

Given the predominant IL-33 expression by FRC within resting LN and its almost exclusive nuclear localization we assessed whether IL-33 regulates transcription in these cells, as well as FRC development, homeostasis, and function. To this end, LN FRC from naive wt and IL-33-deficient mice were compared. First, flow cytometric analysis showed that the composition and number of FRC, LEC and BEC were similar between wild-type, *Il33<sup>gfp/gfp</sup>* and independently generated *Il33<sup>-/-</sup>* mice (Fig. 2A and B; data not shown) with the latter two mouse strains missing the entire exon 2 sequence coding for the N-terminal part of the IL-33 chromatin binding domain. Moreover, the organization and distribution of stromal cells as well as T and B lymphocyte numbers and positioning were comparable in wt, *Il33<sup>gfp/+</sup>*, *Il33<sup>gfp/gfp</sup>* and *Il33<sup>-/-</sup>* mice (Fig. 2C, and data not shown) suggesting IL-33 is dispensable for FRC development and homeostasis. To test whether IL-33 exerts any transcriptional function in FRC, RNA-sequencing was performed on sorted LN FRC from wildtype and *Il33<sup>-/-</sup>* mice. We observed the expected loss of transcripts covering the IL-33 exon 2 which was removed to generate this *Il33<sup>-/-</sup>* mouse model (Supporting Information Fig. 3A). Otherwise no significant differences were observed in gene expression in wt versus *Il33<sup>-/-</sup>* mice (Fig. 2D), including FRC signature genes (Fig. 2E). Together these findings suggest that IL-33 exerts no FRC-intrinsic function in development or homeostasis in two distinct IL-33 deficient mouse strains.

To clarify whether the lack of transcriptional changes in IL-33-deficient mice was specific for LN fibroblasts, we analyzed omental and epididymal adipose fibroblasts that express *Il33* transcripts in wt mice (Supporting Information Fig. 3B). For neither of the two cell types did RNA sequencing reveal any differentially expressed genes in cells isolated from *Il33<sup>-/-</sup>* compared to wt mice. Also, the expression of FRC signature genes was unaltered (Supporting Information Fig. 3C-H). Collectively, our findings argue against an important role of IL-33 in regulating fibroblast development or function in the three tissues studied under homeostatic conditions.

### **Transient loss of IL-33 in lymph node stromal cells early after LCMV clone 13 infection**

IL-33 has a prominent role as an extracellular alarmin by stimulating immune cell activation and proliferation, including during anti-viral CD8<sup>+</sup> T cell responses in the spleen [4, 24]. Currently, we lack a good understanding of the IL-33 expressing cell types during antiviral immune response inside reactive LN, and on how their distribution and IL-33 expression

levels change. To that end, we infected mice intravenously with a high dose of LCMV clone 13 which establishes a non-resolving infection [27, 28], allowing the investigation of the acute and chronic phase of infection, and examined the LN response at several time points. Flow cytometric analysis indicated that FRC did not increase in numbers on day 3, 7 and 14 after clone 13 infection (Fig. 3A), in contrast to published reports on vaccination approaches and herpes simplex virus infection where a roughly 5- to 10-fold FRC expansion has been observed at the peak of the immune response [29-31]. LEC numbers increased 2- or 3-fold on day 3 and 7 after infection, respectively (Fig. 3A), similar to B and T cell numbers (Supporting Information Fig. 4A-B), with BEC numbers increasing approximately 4-fold (Fig. 3A). Flow cytometric analysis of GFP<sup>+</sup> cells confirmed hematopoietic cells remain a poor IL-33 source during infection (Supporting Information Fig. 2C and 4C). Instead, GFP<sup>+</sup> cells were mostly restricted to FRC and LEC (Fig. 3B), similar to naïve LN, and consistent with the reported dependence of the anti-viral T cell response on a non-hematopoietic IL-33 source [4]. The FRC fraction expressing GFP in LN dropped ~2-fold, most prominently between day 3 and day 7 after LCMV clone 13 infection (Fig. 3B) indicating a net loss of IL-33<sup>GFP+</sup> FRC 7 days after infection either due to cell death or reduced GFP reporting. In contrast, the frequency of IL-33<sup>GFP+</sup> LEC remained at ~40% corresponding to a 2-fold increase in absolute numbers of IL-33<sup>GFP+</sup> LEC (Fig. 3A, B). Nevertheless, FRC remained the major IL-33<sup>GFP+</sup> cell population within LN during this time period of LCMV clone 13 infection.

LCMV infection is known to be associated with the transient downregulation of gene transcripts within stromal cells of lymphoid organs, including FRC signature genes [32, 33]. Indeed, the reduction of *Il33* transcripts, as seen both at the level of the GFP reporter and *Il33* mRNA expression during clone 13 infection, was not unique, as other transcripts expressed by stromal cells and FRC in particular were reduced on day 3 p.i., including *Ccl19*, *Ccl21* and *Il7* (Supporting Information Fig. 4D). IL-33<sup>GFP</sup> expression as determined by histology, was reduced on day 3 and day 7 p.i. in all LN compartments typically expressing IL-33 in the naïve steady-state (Fig. 3C, D), which was in line with reduced *Il33* transcription on day 3 p.i.. Importantly, this loss was similarly evident at the level of histologically detectable IL-33 protein, in the T zone, IFR and medulla (Fig. 3C, E). The reduction in IL-33 protein levels was transient as day 14 LN sections showed again a strong and abundant IL-33<sup>GFP</sup> expression in all LN areas, along with a partial restoration of IL-33 protein levels (Fig. 3C-E and Supporting Information Fig. 4E). We postulate that part of this marked loss of

nuclear IL-33 protein should be due to bioactive IL-33 having been released from cells which experienced stress signals or underwent necrosis. The time point of IL-33 depletion from LN tissue coincides with ST2 expression on CD8<sup>+</sup> T cells, which occurs after day 3 and peaks around day 7 after infection (Supporting Information Fig. 4F). This is consistent with previous reports showing ST2 expression peaking on primed CD4<sup>+</sup> and CD8<sup>+</sup> T cells on d4-8 after LCMV-WE infection [4, 5], and thus seems well timed to enable ST2-driven T cell expansion and differentiation by extracellular IL-33.

To test whether LCMV-infected stromal cells preferentially release their stored IL-33 relative to uninfected cells, we investigated the cell tropism and kinetics of LCMV infection within LN. In tissue sections on day 3 p.i., we observed many cells expressing LCMV nucleoprotein (NP) within the IFR, T zone, and to a lesser extent, in the medulla (Fig. 3F, G). Remarkably, these are the same compartments harboring prestored IL-33 protein. On day 7 p.i. NP<sup>+</sup> cells were observed throughout the LN, although at a lower level than on day 3. High-resolution imaging revealed that NP signals were regularly found in proximity of the few remaining IL-33 protein expressing cells, but only occasionally a clear overlap was observed between NP and IL-33 labeling in LN on day 3 with no overlap seen on day 7 or 14 p.i. (Supporting Information Fig 4E).

To define more precisely the potential infection of IL-33<sup>+</sup> LN stromal cells by LCMV clone 13, we performed flow cytometric analysis. FRC were consistently the most frequently infected stromal cell type on day 3 p.i., both in terms of frequency and absolute numbers, closely followed by LEC (Fig. 3H, I and J), comparable to previous findings in the spleen [34]. On average 12% of FRC and 6% of LECs showed NP staining, with most GFP<sup>+</sup> cells being uninfected (Fig. 3H, I). On day 7 p.i. we noted a clear decrease in infected FRC, both in frequencies and absolute numbers, consistent with the histological findings, and possibly pointing to some FRC dying due to necrosis or CTL-mediated killing. The number of infected LEC and BEC increased between day 3 and day 7, reaching levels comparable to FRC. Next, we used flow cytometry to enumerate LCMV-infected IL-33<sup>+</sup> stromal cells, and to look for changes in their frequency of IL-33 expression. On day 3 p.i. only 8% of FRC were NP<sup>+</sup>GFP<sup>+</sup> compared with 60% being NP<sup>-</sup>GFP<sup>+</sup>, whereas on d7 p.i. less than 2% of FRC were NP<sup>+</sup>GFP<sup>+</sup> and 30% were NP<sup>-</sup>GFP<sup>+</sup>. These data suggest that most GFP<sup>+</sup> FRC were not detectably infected but indirectly sensed the infection leading to downregulation of *Il33* mRNA (Fig. 3K). Interestingly, NP<sup>+</sup>GFP<sup>+</sup> FRC were preferentially lost between day 3 and day

7 relative to NP<sup>+</sup>GFP<sup>-</sup> or NP<sup>-</sup>GFP<sup>+</sup> FRC, both in frequencies and numbers (Fig. 3K and L) suggesting a correlation between LCMV infection and *Il33* loss. Similar to FRC, the majority of GFP<sup>+</sup> LEC appear to stay non-infected at these two time-points investigated, while BEC rarely showed IL-33 expression despite some being infected on day 7. To look for a possible correlation between the infection kinetics and *Il33* expression, we performed a statistical mixed model analysis on the histological quantification (Fig. 3D, E and G). This model revealed that the infection day significantly predicts *Il33* expression (P=0.047) and thus suggests an inverse correlation between these two parameters.

Collectively, *Il33* transcripts are downregulated thereby contributing to the decrease in IL-33 protein levels which show similar kinetics. However, these results are also consistent with the notion that at least part of the prestored nuclear IL-33 protein is released into the extracellular space before day 3 after viral infection allowing to stimulate primed ST2<sup>+</sup> T cells found within T zones and/or medullary areas.

### **IL-33 derived from FRC but not LEC drives the anti-viral CD8<sup>+</sup> T cell response to LCMV clone 13**

Previous evidence indicates that during viral infection IL-33 released by splenic stromal cells plays a key role in promoting antiviral CD8<sup>+</sup> T cell responses by signaling via ST2 expressed by these T cells [4, 24]. Therefore, we wished to establish whether this process is similarly IL-33 dependent inside lymph nodes, and to identify the key IL-33 source. First, we examined CD8<sup>+</sup> T cell responses against LCMV clone 13 in peripheral LN of mice lacking IL-33 (*Il33<sup>gfp/gfp</sup>*) by measuring T cell frequencies directed against the two immunodominant LCMV epitopes gp33 and gp276. On day 7 p.i., the frequencies of gp33-tetramer specific T cells were reduced 4-fold in *Il33<sup>gfp/gfp</sup>* versus *Il33<sup>gfp/+</sup>* littermate mice, with absolute numbers showing a more than 2-fold decrease (Fig. 4A and B; Supporting Information Fig. 2B). Frequencies of gp276-tetramer specific T cells were also reduced more than 2-fold in the absence of IL-33 (Supporting Information Fig. 5A). Testing CTL effector functions on day 9 p.i. as a correlate of protective capacity revealed that the number of polyfunctional CD8<sup>+</sup> T cells expressing both IFN $\gamma$  and TNF $\alpha$  was strongly diminished in the absence of IL-33 (Fig. 4C).

To identify the source of stromal IL-33 responsible for driving this antiviral CD8<sup>+</sup> T cell response, we generated two conditional knockout mouse lines in which IL-33 is lacking in either LEC (*Il33<sup>ΔProx1creERT2</sup>*) or FRC (*Il33<sup>ΔCcl19cre</sup>*). To achieve a deletion efficiency of ~90% in Prox1<sup>+</sup> LEC within LN of *Il33<sup>ΔProx1creERT2</sup>* mice, tamoxifen was administered for 2 weeks followed by flow cytometric analysis 3 weeks later (Supporting Information Fig. 4G, H and I). This deletion was LEC-specific as it did not affect intracellular IL-33 protein expression in FRC (Supporting Information Fig. 4I). Analysis of LN in *Il33<sup>ΔProx1creERT2</sup>* mice showed that contrary to global IL-33-deficient mice, the expansion of gp33- and gp276-specific CD8<sup>+</sup> T cells was normal when LEC-derived IL-33 was lacking (Fig. 4D, E and Supporting Information Fig. 5B). Furthermore, IFN $\gamma$  and TNF $\alpha$  production by virus-specific CD8<sup>+</sup> T cells was unaltered in *Il33<sup>ΔProx1creERT2</sup>* mice (Fig. 4F). These results indicate that LEC-derived IL-33 is dispensable for promoting the anti-viral CD8<sup>+</sup> T cell response in LN.

Next, we used *Il33<sup>ΔCcl19cre</sup>* mice to determine the contribution of FRC-derived IL-33 in antiviral T cell responses. The *Ccl19-cre* transgene is known to be highly active in TRC with only a partial activity in MedRC [21, 35, 36]. Indeed, we confirmed this finding by histological analysis of IL-33 expressing FRC with a profound reduction of IL-33 protein signal within the T zone and some remaining IL-33 protein in the medulla, localizing mostly within Lyve-1<sup>+</sup> lymphatic cells (Fig. 4G and H). Deletion of IL-33 in *Ccl19<sup>+</sup>* FRC did not affect the transcriptional expression of FRC signature genes (Supporting Information Fig. 4J) consistent with our previous conclusion of their IL-33 independent development and homeostasis. LN analysis on day 7 p.i. revealed a ~3-fold reduction of Gp33- and Gp276-specific CD8<sup>+</sup> T cells in *Il33<sup>ΔCcl19cre</sup>* mice relative to littermate controls (Fig. 4I and J, and Supporting Information Fig. 5C), with the frequency of polyfunctional CD8<sup>+</sup> T cells expressing both IFN $\gamma$  and TNF $\alpha$  also being strongly reduced in *Il33<sup>ΔCcl19cre</sup>* mice (Fig. 4K). During the chronic phase of clone 13 infection on day 20 p.i., the difference in frequencies and numbers of Gp33- and Gp276-specific T cells was less marked compared to day 7 p.i., but the frequency of cytokine-expressing CD8<sup>+</sup> T cells was strongly reduced in *Il33<sup>ΔCcl19cre</sup>* relative to wt mice (Fig. 4L and Supporting Information Fig. 5D) pointing to long-term consequences of IL-33 deficiency in stroma for T cell function.

Analysis of viremia and spleen virus load showed slightly higher viral titers in *Il33<sup>gfp/gfp</sup>* mice on day 9-14 p.i but these differences were not observed with *Il33<sup>ΔCcl19cre</sup>* mice and their littermate controls (Supporting Information Fig. 5G). In addition, *Il33<sup>gfp/gfp</sup>*, *Il33<sup>ΔProx1creERT2</sup>* and

also *Il33<sup>ΔCcl19cre</sup>* mice eliminated clone 13 infection from blood and spleen by day 70 (Supporting Information Fig. 5E-G). Thus, the decreased T cell response generated in absence of IL-33 was sufficient to eventually contain the virus under the conditions tested here.

### **FRC-derived IL-33 drives also the anti-viral CD8<sup>+</sup> T cell response to acute infection with LCMV WE**

As inoculation with a high dose of LCMV clone 13 establishes an infection which is not efficiently cleared by the immune system, we wished to characterize the role of IL-33 in a second virus infection model where the virus is rapidly eliminated by an efficient effector T cell response [27, 28]. To that end we infected mice with a low dose of the LCMV WE strain which has been previously used to show that in the spleen this infection triggers a transient increase in *Il33* transcript levels along with an IL-33-dependent T cell expansion characterized by ST2 expression by virus-specific T cells on d4-8 p.i. [4, 5]. Indeed, in peripheral LN on d4 and d8 p.i. with LCMV WE, the expression of GFP and IL-33 protein did not decrease but remained virtually unchanged despite the local presence of the virus (Fig. 5A and B; data not shown), very much in contrast to the IL-33 protein loss observed after high dose clone 13 infection. Nevertheless, specific CD8<sup>+</sup> T cells in LN of *Il33<sup>gfp/gfp</sup>* mice at day 8 p.i. with LCMV WE showed a significantly reduced expansion and capacity to co-express IFN $\gamma$  and TNF $\alpha$  compared to *Il33<sup>gfp/+</sup>* littermates (Fig. 5C-E), comparable to the situation with clone 13. While infection of *Il33<sup>ΔProx1creERT2</sup>* mice with WE virus showed no difference relative to wt mice (Fig. 5F-H), *Il33<sup>ΔCcl19cre</sup>* mice infected with LCMV WE showed a pronounced reduction in frequencies and numbers of gp33-tetramer specific cells as well as in the numbers of polyfunctional CD8<sup>+</sup> T cells expressing both IFN $\gamma$  and TNF $\alpha$  (Fig. 5I-K), comparable to the findings in the clone 13 infection model. In summary, while the two LCMV strains differ in their effects on IL-33 expression in reactive LN the results demonstrate that they share the need for IL-33 released by FRC but not LEC to generate a strong CD8<sup>+</sup> T cell response.

## Discussion

In the current study we describe LN FRC as a prominent IL-33 source critical in driving the expansion and differentiation of CD8<sup>+</sup> T cells in response acute and chronic LCMV infection in reactive LN. However, we have not obtained evidence for a nuclear and cell-intrinsic role of IL-33 in FRC of resting LN and fibroblasts at two other sites, despite the abundant expression and nuclear localization of IL-33.

Evidence for a nuclear role for IL-33 has been put forward mainly using cultures of epithelial and endothelial cell lines where IL-33 knockdown strategies led to changes in the expression of selected genes [10-12, 21], with other studies on similar cells coming to the opposite conclusion, including in more global transcriptomic and proteomic approaches highlighting the ST2 dependence of IL-33 mediated effects on transcription [14, 15]. More recently, the first ex vivo study with cells isolated from wildtype and *Il33*<sup>-/-</sup> mice was reported [16]. It indicates a cell-intrinsic role for IL-33 as negative regulator of pro-B cell development and fitness with distinct differences observed at the transcript level. In contrast, our corresponding genome-wide transcriptional comparison on FRC isolated from resting LN as well as two other fibroblast subsets did not reveal any difference, although the same exon 2 coding sequence had been removed by gene targeting as in the pro-B cell study cited above. Our failure to detect transcriptional differences corroborated with unaltered FRC numbers, phenotype and network organization in two different *Il33*<sup>-/-</sup> mouse lines as well as in FRC-specific IL-33 knockout mice, suggesting fibroblast development and homeostasis occurs normally in absence of nuclear IL-33. This conclusion is supported by other studies reporting grossly normal organization and homeostatic function of tissues expressing high IL-33 levels [7, 25]. So far, most deficiencies described for the various IL-33<sup>-/-</sup> mouse strains available are thought to be due to the extracellular cytokine signaling via ST2<sup>+</sup> immune cells and become apparent only upon immune stimulation and/or metabolic changes [1-3]. These deficiencies observed seem to be independent of the IL-33<sup>-/-</sup> mouse model used that either remove the N- or C-terminal part of IL-33 protein. At present, we cannot fully rule out a role for a short nuclear IL-33 form that is not recognized by the polyclonal antibody directed against the C-terminal half of the IL-33 protein and used by several laboratories, both for western blot and histological analysis (Figure 1) [7, 25]. Also, we cannot exclude a

transcriptional role of IL-33 in FRC during the very early or late phase of immune response when nuclear IL-33 protein is detectable in FRC. However, the current data are in agreement with the interpretation that IL-33 is localized in the nucleus of FRC and other fibroblast types for storage purposes rather than transcriptional regulation. Nuclear retention of IL-33 may be a safety measure to prevent leakiness from cytoplasmic compartments given the strong proinflammatory effects of this cytokine, while allowing the rapid release upon cell damage or stress [3, 37]. In addition, the chromatin association of IL-33 may help to delay release of the cytokine thereby prolonging its proinflammatory effect [3, 15].

Here we show that FRC and LEC are the main IL-33 source in naïve and virus-activated LN with FRC, but not LEC or hematopoietic cells, being critical in mounting the antiviral T cell response. At first glance, it may surprise that LN FRC have a prominent role as IL-33 source in adaptive immunity. While distant from epithelial barriers where pathogens typically enter, LN are directly associated with sites of infection and inflammation by collecting interstitial fluid generated in pathogen-invaded tissues. Afferent lymphatic vessels transport interstitial fluid carrying pathogens, inflammatory cytokines, and antigen-presenting cells to LN. As such, LN are strategic sites for generating immune responses against tissue-derived pathogens, most notably the T zone where DC trigger clonal selection and amplification of antigen-specific T cells. Here we show that within the LN T zone there are Pdpn<sup>+</sup> FRC, which are known to form a specialized network for attracting and retaining DC and T cells, and that constitutively express high levels of preformed nuclear IL-33 protein prior to pathogen arrival (Fig. 6)[6, 7]. Similar to CCL19 and CCL21 [22], there is some heterogeneity among FRC for IL-33 expression, with more than 70% being IL-33<sup>+</sup>, consistent with recent reports highlighting the existence of several transcriptionally distinct LN FRC subsets [18]. Importantly, DC that provide the antigenic stimulation (signal 1) along with co-stimulation (signal 2) and cytokines (signal 3) to Ag-specific T cells are not a relevant source of IL-33 for T cell responses but it is a stromal source as in other immune reactions and diseases [1-3]. Consistent with this notion, primed T cells upregulate ST2 expression only later, peaking after day 3 [4], when they are only infrequently interacting with DC but are in a vigorous proliferation phase [38]. Therefore, we postulate the initial CD8<sup>+</sup> T cell expansion is likely to be IL-33 independent with IL-33 signals from FRC strongly enhancing the later T cell expansion occurring around day 3-8 (Fig. 6). During this second phase the expanding T cells still localize to the T zone and are thought to be in continuous contact with TRC that form a

migration scaffold for naive and activated T cells [39]. We propose therefore that T zone FRC are proinflammatory cells in this phase of the response and provide this key signal to further expand selectively the activated T cells and enhance their differentiation into effector cells. During the chronic phase of the response, FRC-derived IL-33 allows CD8<sup>+</sup> effector T cells to augment their cytokine expression level, or to drive the differentiation process from memory-like CD8<sup>+</sup> T cells to effector cells. This scenario is likely to be comparable in the spleen where T zone FRC are the prominent IL-33 source in LCMV infection [4, 24] with the presence of only rare lymphatic vessels. It remains to be determined what the precise role of IL-33 is within LN lymphatic vessels and why there is only a subset expressing IL-33.

Despite the marked difference in T cell expansion and effector function in wt versus *Il33*<sup>-/-</sup> mice, both in the early and later phase of clone 13 infection, it did not impact virus control under the conditions tested. This is consistent with observations of comparable viremia in wt versus *ST2*<sup>-/-</sup> mice in the first 10 or 40 days after infection with LCMV-WE or clone 13, respectively [4]. However, in that study *ST2*<sup>-/-</sup> mice did not clear clone 13 after day 40, contrary to wt mice, while in the current study the virus was eventually cleared in both wt and *Il33*<sup>-/-</sup> mice. At present we can only speculate about the reasons for this variability that may include differences in the virus stock or effective titer used, or in the mouse model and colony studied. We conclude that the T cell mediated virus eradication is not in all settings IL-33-dependent, either because there are alternative or compensatory mechanisms at play, or because the reduced T cell immunity is still sufficient in controlling the virus. Similar conclusions have been reached for Th2 responses to parasite infections [1, 2]. It should be kept in mind, however, that in some responses to infections IL-33 makes a critical difference in pathogen control by accelerating and augmenting innate and adaptive immunity [1, 2, 4].

The signals leading to IL-33 release by FRC are currently unclear, as is the cellular process allowing this release. Several studies on other IL-33 expressing cell types suggest a role for DAMP, mechanical stress, or necrosis-inducing signals as initial triggers, with cells typically undergoing necrosis or necroptosis [1-3, 40]. We observed a marked loss of IL-33 protein from most of the T zone on day 3-7 p.i. with clone 13, but FRC numbers and network organization remained largely preserved. While we cannot exclude the possibility that stromal cells proliferate and compensate for dying cells, our findings rather argue against

extensive stromal cell death. After infection with LCMV-WE, no major loss of IL-33 expressing cells was detectable, suggesting again that the FRC network remains largely intact during this early phase of viral infection when IL-33 is released. We therefore postulate that FRC stay alive when releasing IL-33, as shown previously fibroblasts and myocytes upon application of mechanical strain [41]. Possibly, virus-induced inflammation leads to increased lymph drainage via conduits that FRC are lining thereby leading to mechanical stress induced IL-33 release from live cells thereby preserving the critical LN architecture.

LCMV is a non-lytic virus and damage to the FRC network, as described previously for the spleen, is mainly due to T-cell mediated elimination of virus-infected FRC once effector cells have been generated [32, 34], with apoptosis of IL-33 expressing cells leading to protease-mediated inactivation of this alarmin [1-3]. Recently, viral infection of an epithelial cell line was suggested to provoke IL-33 release, with indirect evidence also from virus-infected lungs [42]. At present we cannot exclude that a small number of IL-33 expressing FRC undergo necroptosis [40], possibly after having been infected. To test whether only LCMV-infected cells lose IL-33 expression, we have measured the fraction of infected FRC during the presumed IL-33 release phase around day 3 after clone 13 infection. The FRC-infection frequency with clone 13 we observed in LN was low with a small fraction of IL-33<sup>+</sup> FRC being infected, despite the injection of a high virus dose. This result is consistent with a previous study for low dose WE infection in the spleen [24]. These findings support the notion that FRC do not necessarily need to be infected to release or downregulate IL-33. Rather, FRC are able to sense the infection also in neighboring cells, possibly via recognition of DAMP released by infected cells or due to signals exchanged between neighboring FRC via gap junctions. FRC do not express *St2* mRNA in the resting state [8] suggesting IL-33 released from neighboring infected cells is not acting upstream. Intriguingly, only replicating but not non-replicating viruses trigger the IL-33-dependent CD8<sup>+</sup> T cell expansion process [4, 24]. The identification of the pathway induced by replicating viruses will be an interesting avenue for future research with high relevance for antiviral immunity as well as for vaccine development. Our study here suggests that this process should be studied within LN FRC that we have identified here as the key drivers of the IL-33 driven process of antiviral CD8<sup>+</sup> T cell expansion and effector differentiation.

## Acknowledgments

We thank Karin Schaeuble, Leonardo Scarpellino, Leonor Morgado, Katambayi Muamba Kamanda, Wilson Castro, Loriane Savary (University of Lausanne), and Min Lu (University of Basel) for technical help. Hirohisa Saito (National Research Institute for Child Health & Development, Tokyo, Japan) and Yasuhide Furuta (LARGE, RIKEN BDR- RIKEN Center for Biosystems Dynamics Research, Kobe, Japan) for allowing to use their  $I33^{-/-}$  mice and R.T. Lee (Harvard University, Boston, USA) for  $I33^{flox/flox}$  mice, Taija Mäkinen (Uppsala University, Sweden) and Tatiana Petrova (University of Lausanne) for sharing Prox1-creERT2 mice, Doron Merkler (University of Geneva, Geneva, Switzerland) and Max Löhning (Charité, Universitätsmedizin Berlin, Germany) for critical discussions and sharing tools; Stokes Peebles for critical reading of the manuscript. This project has received funding from the European Union's Horizon 2020 research and innovation program under the Marie Skłodowska-Curie grant agreement (No 708715 to PAD) and by the Swiss National Science Foundation Sinergia program (CRSII3\_160772 to D.D.P. and S.A.L.) and an individual SNF grant (166500 to B.L.). We thank the mouse, microscopy and flow cytometry facility at the University of Lausanne; the Genentech animal core groups for animal care and genotyping analysis, and the Genentech core facility staff for bioinformatics assistance.

Author contributions: PAD, SAL, MBB and SJT conceived and designed research, and interpreted the data. PAD, HC, MBB, SN, SF and NP conducted experiments, acquired and analyzed data; SMK and DDP provided reagents, training and preliminary experiments; BL provided reagents; TC organized and interpreted the human tissue analysis; PAD and SAL assembled the first manuscript draft; and all authors read, critically commented on, and approved the manuscript.

**Conflict of interest:** the authors declare no commercial or financial conflict of interest.

## Material and methods

## Mice

*Il33<sup>gfp/gfp</sup>* mice obtained through the RIKEN Center for Developmental Biology (Acc. No. CDB0631K) [25] have a GFP replacing the N-terminus of the *Il33* coding sequence in exon 2; they were crossed to the ZP3-cre germline deleter strain to remove the neomycin cassette [24], before intercrossing them or crossing them to C57BL/6JOlaHsd from Envigo (Netherlands) to obtain *Il33<sup>gfp/gfp</sup>* and *Il33<sup>gfp/+</sup>* mice, respectively. *Il33<sup>lox/lox</sup>* mice [43] were crossed with *Ccl19-Cre* [35] or *Prox1-CreERT2* [44] mice, all on a C57BL/6J background, to delete in a cell-type-specific fashion exons 5-7 of IL-33 which code for most of the cytokine domain.

All RNA sequencing experiments were performed on a second *Il33<sup>-/-</sup>* mouse model: A conditional knock-out allele of the exon 2 of *Il33* on the C57BL/6N background was generated by GenOway, France. Mice with the *Il33* knock-out allele were subsequently generated at Genentech by a cross to a ROSA26-Cre mouse line. The 1067 bp floxed region included the first translated exon (exon 2) and has the following genomic coordinates: chr19:29,948,795-29,949,861 (GRCm38/mm10). The absence of exon 2 correlated with no IL-33 protein detectable in lymphoid organs by ELISA (data not shown) consistent with the previous demonstration that deletion of exon 2 leads to lack of IL-33 protein detection in lung by Western blot [25]. All mice were maintained in pathogen-free conditions and were age and sex matched for experiments. All mouse experiments were authorized by the Swiss Federal Veterinary Office (for the Luther lab; VD 3196) or Genentech (for the Turley lab).

## RNA sequencing and bioinformatics analysis.

Male *Il33<sup>-/-</sup>* or littermate control mice 7–19 weeks old were used for RNA-Seq experiments. Each fibroblast sample (n = 3 littermate control and 3 *Il33<sup>-/-</sup>* per tissue) was derived by pooling cells from 4-5 mice and FACS-sorting CD45<sup>-</sup>EpCAM<sup>-</sup>CD31<sup>-</sup>Pdpr<sup>+</sup>PDGFR $\alpha$ <sup>+</sup> cells. For each sample, 19,000-100,000 cells were sorted at >94% purity directly into Trizol (Thermo Fisher Scientific). RNA was isolated at Expression Analysis, Inc.. All samples had RIN scores of greater than 7, as determined with a BioAnalyzer (Agilent).

Paired-end RNA-Seq libraries were constructed from 2ng of RNA using the SMARTer Ultra Low Input kit (Clontech). Libraries were sequenced on an Illumina HiSeq yielding, on

average, 33.9 million read pairs (2x50bp) per sample. Transcript-level quantification was performed with Salmon version 0.6 [45] against the GENCODE M9 mouse transcript models with parameters set to "-l IU" for library type and "--biasCorrect". Gene level expression was estimated using the tximport R package [46]. Differential expression tests were performed with voom/limma [47].

### **LCMV infection and tamoxifen treatment**

LCMV clone 13 and WE virus stocks were generated according to an established protocol [48]. LCMV clone 13 was administered at a dose of  $2 \times 10^6$  PFU and WE at a dose of 200 PFU, both intravenously. Tamoxifen (Sigma) was diluted in sunflower seed oil (Sigma) and administered intraperitoneally at 0.05mg/g of weight per day, for 3 days per week, during 2 weeks (as shown in Supporting Information Fig. 4G).

### **Stromal and hematopoietic cell isolation**

LN stroma isolation was performed as previously described [21]. Briefly, axillary, brachial and inguinal LN were cut into small pieces and digested for 30 min at 37°C with gentle stirring in 1.5 ml DMEM medium (Gibco) containing collagenase IV (3 mg/ml; Worthington), DNase I (40 µg/ml; Roche),  $\text{CaCl}_2$  (3 mM) and 2% (vol/vol) FCS. Cells were passed through a 40 µm strainer (Becton Dickinson), washed twice and resuspended in DMEM/2% FCS. When stromal cells were not required, single cell suspensions of hematopoietic cells were prepared by meshing LN through a 70 µm cell strainer. Red blood cells were lysed with a Tris-Ammonium chloride-based buffer.

### **Peptide re-stimulation**

Lymphocytes from LN of LCMV-infected animals were isolated and  $2 \times 10^6$  cells were seeded per 96-well. Cells were stimulated *in vitro* with 1µM of gp33, gp276 and np396 peptides (EMC Microcollections) for 4h at 37°C. 30 minutes after peptide re-stimulation Brefeldin A (10 µg/ml, AppliChem) was added to the culture medium. After 4h of incubation at 37°C, cells were harvested, washed and stained for surface or intracellular epitopes followed by analysis using flow cytometry. Endogenous  $\text{CD8}^+$  T cells specific for LCMV were labelled

with APC or PE conjugated peptide-MHC tetramers (Db /gp33-41; TC Metrix) for 90min at 4°C.

### Flow cytometry

Cells were blocked with anti-CD16/32 antibody (2.4G2) and then stained for 30 min at 4°C using the following fluorochrome-coupled antibodies to CD45pan (30-F11), CD45R/B220 (RA3-6B2), CD8 $\alpha$  (53-6.7), CD4 (H129.19.6) and Pdpn (8.1.1) antibodies have been generated in house. Or with the following commercial antibodies to: CD31 (390) from Biolegend; IFN $\gamma$  (XMG1.2), TNF $\alpha$  (MP6-XT22), TCR $\beta$  (H57-597) from eBioscience; CD19 (ID3) from BD Biosciences; IL-33 (AF3626) from R&D Systems. For intracellular staining of IFN $\gamma$  and TNF $\alpha$ , cells were fixed and permeabilized using the Cytofix/Cytoperm kit (Becton Dickinson). For intracellular staining of IL-33, the True-Nuclear Transcription Factor Staining buffer and protocol (BioLegend) was used. For surface ST2 antibody staining (DJ8, MD Bioproducts), two rounds of amplification were carried out with PE-Faser Kit (Miltenyi Biotec) according to the manufacturer's instructions. Dead cells were excluded by marking them with the Fixable Aqua Dead Cell Staining Kit (Invitrogen). Data were acquired on a LSRII (BD Biosystems) and analyzed with FlowJo 2 (TreeStar). Full gating strategy is shown in Supporting Information Fig. 2.

### Quantitative Realtime PCR

Whole LN (pool of axillary, brachial and inguinal LN) samples were homogenized in TRIzol (Ambion, life technologies) by bead beating for subsequent RNA extraction. First-strand cDNA synthesis, quantitative real-time PCR, and normalization are as described previously [23]. RNA of sorted cells was isolated using RNeasy Micro Kit (Qiagen). Sequences of primer pairs used are as follows:

*Hprt*: Fwd: 5'- GTTGATATGCCCTTGAC-3' and Rev: 5'-AGGACTAGAACACCTGCT-3';  
*Tbp*: Fwd: 5'- CCTTCACCA ATGACTCCTATGAC-3' and Rev:5'-  
CAAGTTTACAGCCAAGATTCAC-3'; *I17*:Fwd:5' GTGCCACATTAAGACAAAGAAG-3' and  
Rev: 5'GTTTCATTATTCGGGCAATTACTATC-3'; *I133*: Fwd: 5'-  
TCCAACCTCCAAGATTTCCCCG -3' and Rev: 5'- CATGCAGTAGACATGGCAGAA-3'; *Cd19*:  
Fwd: 5'- CTGCCTCAGATTATCTGCCA -3' and Rev: 5'-AGGTAGCGGAAGGCTTTTCAC-3';

21

*Ccl21*: Fwd: 5'- ATCCCGGCAATCCTGTTCTC -3' and Rev: 5'- GGTTCCTGCACCCAGCCTTC-3'; *Cxcl12*: Fwd: 5'- TGCATCAGGGTAAACCA -3'; Rev: 5'- TTCTTCAGCCGTGCAACAATC -3' *Baff*: Fwd: 5' AGACGCGCTTTCCAGGGACC -3' and Rev: 5' TAGTCGGCGTGTCGCTGTCTG-3' and *Col1a*: Fwd: 5' GTAACCTTCGTGCCTAGCAACA -3' and Rev: 5' CCTTTGTCAGAATACTGAGCAGC -3'

### Immunofluorescence and image acquisition

Murine tissues were fixed in 2% PFA for 4 hours and subsequently incubated overnight in 30% sucrose before embedding in Tissue-tek OCT. Cryosections were cut at 8  $\mu$ m and immunostaining was performed using antibodies. Primary antibodies against murine proteins were specific for CD3 (145-2c11), CD31 (GC-51), B220 (RA3-6B2), Podoplanin (8.1.1) and have been generated in house; antibodies to Lyve-1 (103-PA50, RELIA Tech), IL-33 (AF3626, R&D Systems), BP3/CD157 (140-206) and GFP (A11122; both from Life technologies), NP-LCMV (VL-4) hybridoma supernatant provided by D. Pinschewer. Additional secondary labeling reagents were donkey-anti-rabbit IgG -Alexa488 and -Alexa647 (both Life technologies) -Cy3 (Jackson ImmunoResearch), donkey-anti-rat IgG -Cy3 (Jackson ImmunoResearch), goat-anti-Syrian hamster IgG -Cy3 (Jackson ImmunoResearch) and donkey-anti-goat IgG -Alexa647 (ThermoFisher).

Human tissues were obtained from patients with their informed consent and with permission granted by the Ethical committee of the Erasmus Medical Center (number: MEC-2014-060). OCT- embedded tissues were sectioned and fixed in acetone. Antibodies against human proteins were specific for IL33 (MAB36252, R&D systems), Lyve-1 (ab36993, Abcam), Podoplanin (D2-40, BioLegend), MadCAM (314G8, Hycult Biotech), CD31 (WM-59, eBioscience) and CD35 (UJ11, Immunotools).

Images were acquired with an upright Zeiss Axiovision microscope. Images were treated using Fiji (NIH) or Adobe Photoshop. Exposure and image processing were identical for mouse groups which were directly compared.

### Statistics

For statistical analysis, GraphPad Prism software (Version 7.0, GraphPad Software) was used. Unpaired two-tailed student's test was performed to compare two groups while single values of multiple groups were compared by one-way analysis of variance (ANOVA). Linear regression mixed effects analysis with time as a random effect, combined with ANOVA was performed on LCMV kinetic assays. P values were considered significant if  $P \leq 0.05$  (\*) or if  $P \leq 0.01$  (\*\*) and highly significant if  $P \leq 0.001$  (\*\*\*) .

## Figure legends

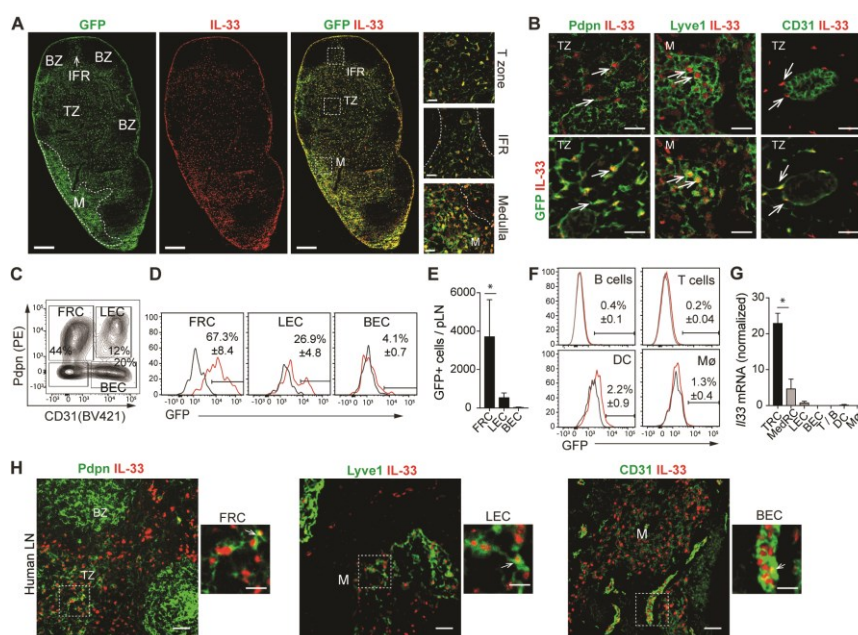


**Figure 1. FRC and endothelial cells are the main IL-33 producers in murine and human LN.** (A-B) Immunofluorescence labeling of naïve peripheral lymph node (pLN) sections from *Il33<sup>gfp/+</sup>* mice. (A) Labeling of GFP (green) and of IL-33 protein (red) derived from the GFP knock-in and wt IL-33 alleles, respectively. GFP is a reporter for IL-33 promoter activity and *Il33* transcription. Higher magnification of T zone (TZ), interfollicular region (IFR) in between B zones (BZ), and medulla (M) revealing co-localization of GFP and IL-33 protein in yellow. Scale bar represents 200µm in whole LN images and 20µm in magnified areas. (B) Higher magnification images showing IL-33 protein (red) expressing cells: Pdpn<sup>+</sup> FRC (green) in T zone, Lyve1<sup>+</sup> LEC (green) within the medullary sinus and non-endothelial cells adjacent to CD31<sup>+</sup> HEV (green). The row below shows the same region for

GFP (green) and IL-33 protein (red) expression. Scale bar represents 20 $\mu$ m. **(C-G)** Flow cytometric analysis of stromal cells from naïve LN of *Il33<sup>gfp/+</sup>* mice. **(C)** Gating strategy for FRC (Pdpn<sup>+</sup>CD31<sup>-</sup>), LEC (Pdpn<sup>+</sup> CD31<sup>+</sup>) and BEC (Pdpn<sup>-</sup> CD31<sup>+</sup>) among CD45<sup>-</sup> cells. **(D)** Representative histograms showing the frequency of GFP<sup>+</sup> cells within each stromal subset in LN of *Il33<sup>gfp/+</sup>* (red line) compared to wt control mice (black line). **(E)** Number of GFP<sup>+</sup> cells within the indicated stroma subsets. **(F)** Frequency of GFP<sup>+</sup> B cells, T cells, dendritic cells (DC) and macrophages (M $\phi$ ) in *Il33<sup>gfp/+</sup>* (red line) compared to wt control mice (black line). **(G)** Levels of *Il33* transcripts in the indicated cells sorted from naïve LN were measured by RT-qPCR and normalized against *Hprt* and *Tbp1*. **(H)** Immunofluorescence staining of human hepatic LN sections for IL-33 protein expressing regions and cell types, including T zone FRC (Pdpn<sup>+</sup>), medullary sinus LEC (Lyve1<sup>+</sup>, CD31<sup>low</sup>) and T zone BEC (CD31<sup>high</sup>). Scale bar represents 50  $\mu$ m in LN images and 20 $\mu$ m in magnifications. Data are representative examples of 2-3 independent experiments (**A-F**) (n=2-3 mice per group) or 1 experiment (**G**) (n=4). Data are expressed as mean  $\pm$  SEM. Unpaired *t*-test \*P < 0.05

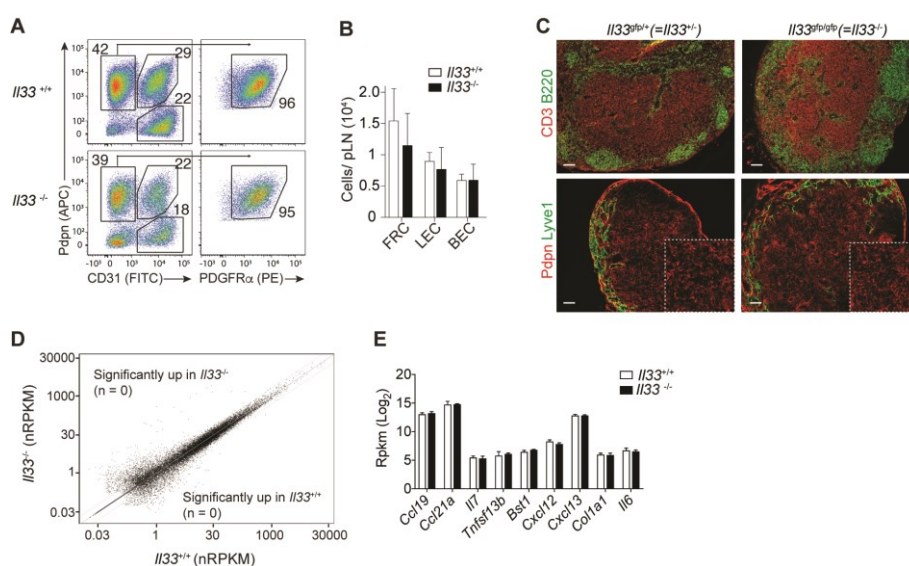


**Figure 2. IL-33 is dispensable for LN FRC development, homeostasis and gene expression. (A-B)** Flow cytometric characterization of CD45<sup>+</sup>EPCAM<sup>-</sup> stromal cells from naïve LN of wt versus *Il33<sup>-/-</sup>* mice: FRC (Pdpn<sup>+</sup>CD31<sup>-</sup>PDGFR $\alpha$ <sup>+</sup>), BEC (Pdpn<sup>-</sup>CD31<sup>+</sup>), LEC (Pdpn<sup>+</sup>CD31<sup>+</sup>). Representative flow cytometry dot plots with relative frequencies (**A**) and absolute cell numbers (**B**). **(C)** Histological analysis of naïve LN from *Il33<sup>+/+</sup>* (= *Il33<sup>gfp/+</sup>*) versus *Il33<sup>-/-</sup>* (= *Il33<sup>gfp/gfp</sup>*) mice showing normal B (green) and T lymphocyte (red) distribution (upper panel), Pdpn<sup>+</sup> lyve-1<sup>-</sup> (red) FRC networks in T zone and lyve-1<sup>+</sup> (green) medullary lymphatic

vessels (lower panel). Scale bar represents 100 $\mu$ m. **(D-E)** Flow cytometry sorted wt and *Il33*<sup>-/-</sup> FRC from naive LN analyzed by RNA-sequencing for differentially expressed genes (false discovery rate (FDR)  $\leq$  0.05, Fold change (Log2)  $\geq$  2) **(D)** and the expression of canonical FRC genes **(E)**. nRPKM: normalized read per kilobase of transcript per million mapped reads. All data are representative examples of 2-3 independent experiments with 2 **(C)** or 3 **(A-B, D-E)** mice per group. Data are expressed as mean  $\pm$  SEM. Unpaired *t*-test (B, E), voom/limma test (D).

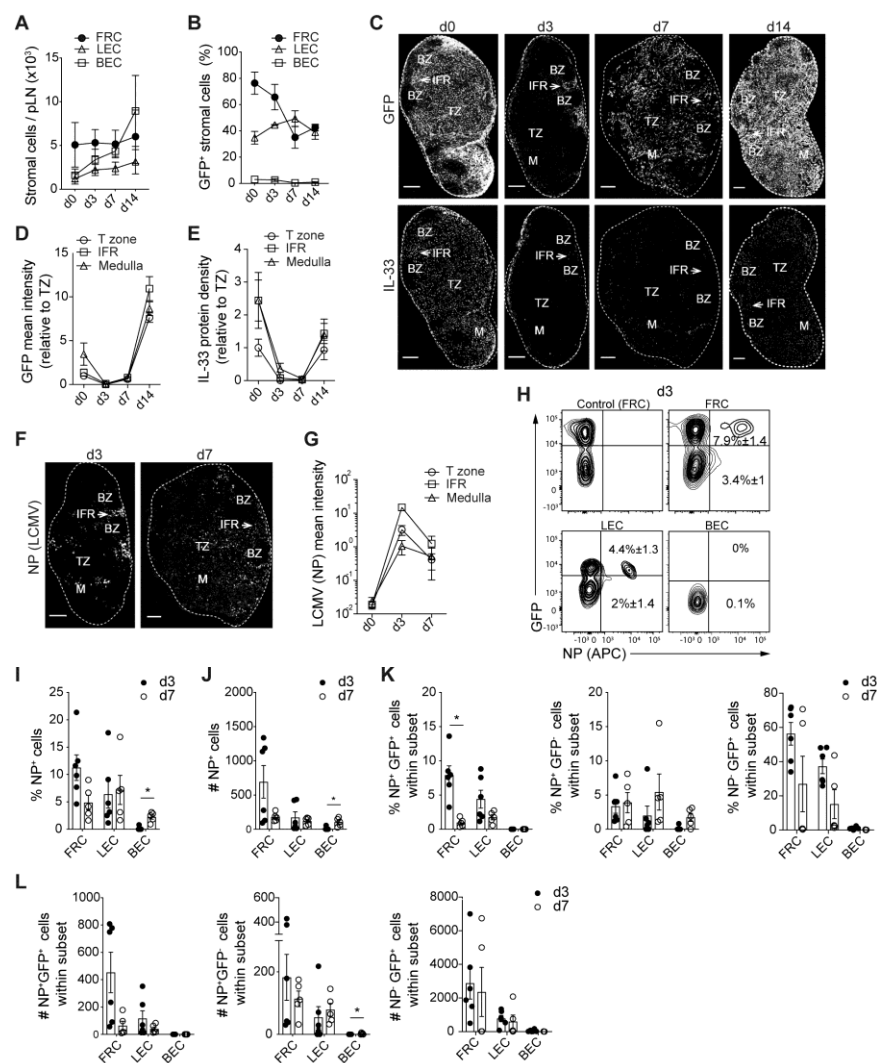


**Figure 3. Transient loss of IL-33 transcripts and protein in LN stromal cells early after LCMV clone 13 infection.** Shown are analysis of pLN from *Il33*<sup>gfp/+</sup> mice at the indicated days (d) after infection. **(A-B)** Flow cytometric analysis of the three major stromal cell types: Kinetics of cell numbers **(A)** and frequencies of GFP<sup>+</sup> cells per subset **(B)**. **(C)**

Immunofluorescence staining of LN cross-sections for GFP and IL-33 protein expression. Scale bars represent 200 $\mu$ m. **(D-E)** Quantification of immunofluorescence staining, as shown in D, for GFP intensity and IL-33 protein density per indicated area. T zones (TZ), interfollicular regions (IFR) and medullary regions (M) were distinguished using DAPI co-staining and all data were normalized to TZ d0 data. **(F-G)** Representative examples of immunofluorescence staining showing viral nucleoprotein (NP) expression as surrogate marker for LCMV infection **(F)** and the quantification for NP intensity per region **(G)**. BZ: B zone. Scale bar represents 200 $\mu$ m. **(H-K)** Flow cytometric analysis of LCMV-infected stromal cell subsets. **(I)** Representative flow cytometry contour plots depicting the frequency of NP<sup>+</sup> stromal cells as based on intracellular NP labeling. Shown as control is the staining of FRC from an uninfected LN. **(I-J)** Frequencies **(I)** and cell numbers **(J)** of NP<sup>+</sup> stromal cells. **(K-L)** Frequencies **(K)** and cell numbers **(L)** of NP<sup>+</sup> cells among the GFP<sup>+</sup> versus GFP<sup>-</sup> stroma subsets measured by flow cytometry. All data are pooled or are representative examples (C and F) from 2 independent experiments (n=2-3 per group). Data are expressed as mean  $\pm$  SEM. ANOVA Bonferroni-Sidak test, \*P < 0.05

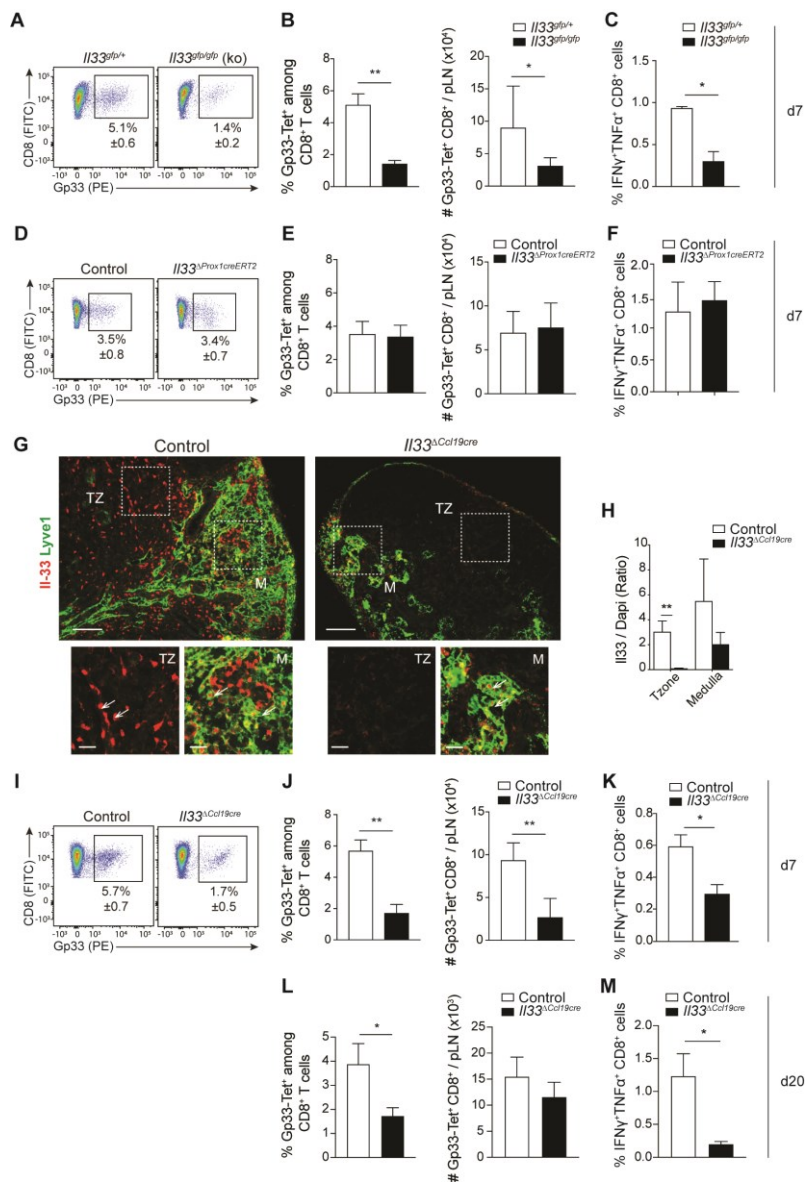


**Figure 4. IL-33 derived from FRC but not LEC strongly augments the CD8<sup>+</sup> T cell response against clone 13 infection. (A-C)** Flow cytometric analysis of CD8<sup>+</sup> T cells from peripheral LN of *I133<sup>gfp/+</sup>* and *I133<sup>gfp/gfp</sup>* (corresponding to *I133<sup>-/-</sup>*) littermate mice on day 7 after LCMV clone 13 infection. Representative density plots showing LCMV-specific CD8<sup>+</sup> T cells labeled with Gp33-Tetramers (Tet) **(A)**, with bar graphs showing their frequencies and absolute numbers **(B)**. **(C)** Frequency of CD8<sup>+</sup> T cells producing intracellular IFN $\gamma$  and TNF $\alpha$  protein, upon restimulation in vitro with viral peptides followed. **(D-F)** Identical analysis as in **(A-C)** but for CD8<sup>+</sup> T cells from mice lacking IL-33 specifically in LEC (*I133<sup>ΔProx1creERT2</sup>*) versus their Cre-negative littermate controls on d7 p.i.. **(G-H)** Validation of successful IL-33 deletion in T zone FRC of naïve LN in *I133<sup>ΔCcl19cre</sup>* versus control littermate mice. **(G)** Representative microscopic images of IL-33 protein (red) staining in medulla (M) and T zone (TZ) areas

identified by lyve-1 (green) and DAPI staining, respectively (DAPI is not shown). Scale bar represent 100 $\mu$ m in the upper panel and 20 $\mu$ m in the magnifications. **(H)** Histological quantification showing the ratio of IL33<sup>+</sup> versus DAPI<sup>+</sup> nuclei in T zones versus medullary areas. **(I-K)** Identical analysis as in **(A-C)** but for CD8<sup>+</sup> T cells from mice lacking IL-33 specifically in FRC (*Il33 $\Delta$ Ccl19<sup>cre</sup>*) versus their Cre-negative littermate controls on day 7 and day 20 p.i. (L and M). All data are representative of 2 independent experiments (n=3-5 per group). Data are expressed as mean  $\pm$  SEM. Unpaired *t*-test \*P < 0.05.

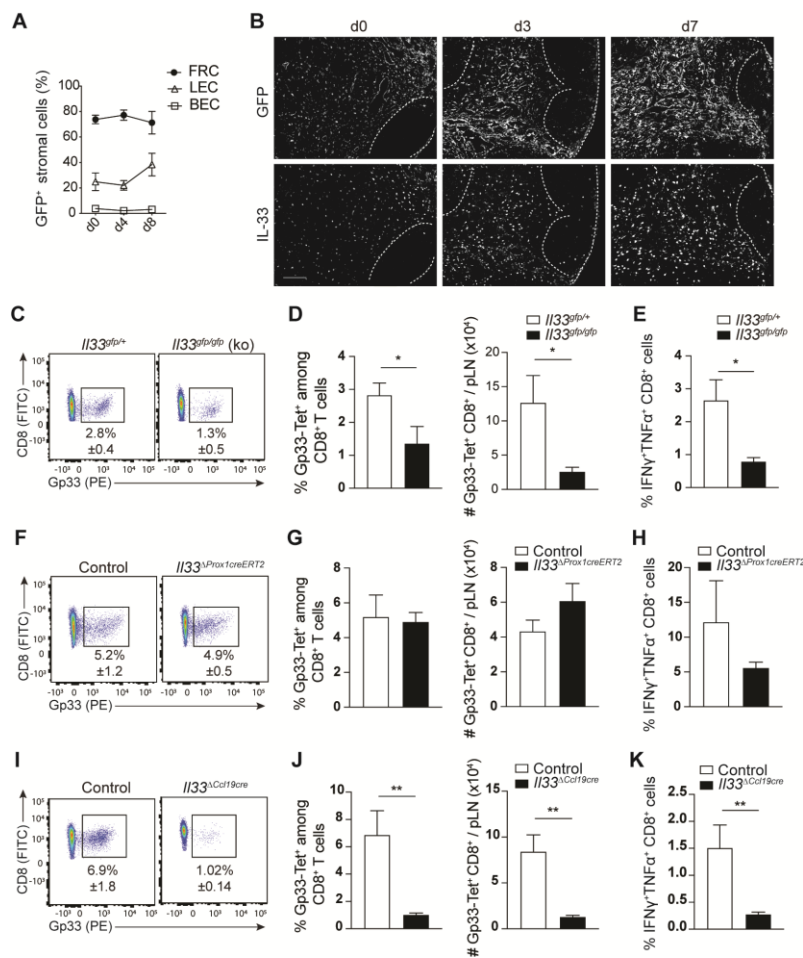


**Figure 5. The acute CD8<sup>+</sup> T cell response triggered by LCMV WE infection is also dependent on IL-33 provided by FRC but not LEC. (A)** Flow cytometric analysis of the three major stromal showing the frequencies of GFP<sup>+</sup> cells per subset at the indicated time points after LCMV WE infection. **(B)** Immunofluorescence staining of LN cross-sections for GFP and IL-33 protein expression at the indicated time points after LCMV WE infection.

Scale bars represent 100 $\mu$ m. **(C-E)** Flow cytometric analysis of CD8<sup>+</sup> T cells from pLN of *Il33<sup>gfp/+</sup>* and *Il33<sup>gfp/gfp</sup>* (corresponding to *Il33<sup>-/-</sup>*) mice at day 8 after LCMV WE infection. **(C)** Representative flow cytometry plots showing LCMV-specific CD8<sup>+</sup> T cells labelled with Gp33-Tetramers. **(D)** Gp33-Tetramer<sup>+</sup> CD8<sup>+</sup> T cell frequencies and absolute numbers. **(E)** Frequency of CD8<sup>+</sup> T cells producing IFN $\gamma$  and TNF $\alpha$ , upon restimulation in vitro with viral peptides followed by intracellular cytokine staining. **(F-H)** Flow cytometric analysis of CD8<sup>+</sup> T cells from mice lacking IL-33 specifically in LEC (*Il33 $\Delta$ Prox1creERT2*) versus their Cre-negative littermate controls at day 8 after LCMV WE infection. **(F)** Representative flow cytometry plots showing LCMV-specific CD8<sup>+</sup> T cells labelled with Gp33-Tetramers. **(G)** Frequencies and absolute cell numbers of Gp33-Tetramer<sup>+</sup> CD8<sup>+</sup> T cells. **(H)** Frequency of CD8<sup>+</sup> T cells producing IFN $\gamma$  and TNF $\alpha$ , upon restimulation in vitro with viral peptides followed by intracellular cytokine staining. **(I-K)** Flow cytometric analysis of CD8<sup>+</sup> T cells from mice lacking IL-33 specifically in FRC (*Il33 $\Delta$ Ccl19cre*) versus their Cre-negative littermate controls at day 8 after LCMV WE infection. **(I)** Representative dot plots showing LCMV-specific CD8<sup>+</sup> T cells labelled with Gp33-Tetramers. **(J)** Frequencies and absolute cell numbers of Gp33-Tetramer<sup>+</sup> CD8<sup>+</sup> T cells. **(K)** Frequency of CD8<sup>+</sup> T cells producing IFN $\gamma$  and TNF $\alpha$  upon peptide restimulation. All data are representative of 2 independent experiments (n=2-4 mice per group). Data are expressed as mean  $\pm$  SEM. Unpaired *t*-test \*P <0.05.

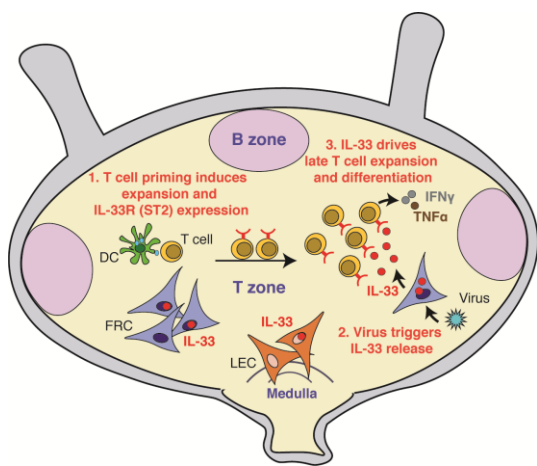


**Figure 6. Model for CD8<sup>+</sup> T cell expansion and differentiation driven by IL-33 released by FRC in LN T zones during LCMV infection.** Early after infection, dendritic cells expressing viral peptides in the context of MHC class I and costimulatory signals prime CD8 T cells within the T zone, leading to their rapid expansion and their expression of the IL-33

receptor (ST2). Ccl19Cre<sup>+</sup> FRC in the T zone have IL-33 protein prestored in the nucleus and release this 'alarmin' cytokine into the extracellular space upon sensing of stress signals derived from the viral infection. The secreted IL-33 drives the later expansion of the neighboring ST2-expressing CD8 T cells around day 4-8 after infection and thereby considerably enhances the anti-viral CTL response. While LEC can express nuclear IL-33 no limiting role could be identified in this viral infection model, possibly because T cells show less frequent contacts with medullary lymphatic vessels.

## References

- 1 **Molofsky, A. B., Savage, A. K. and Locksley, R. M.**, Interleukin-33 in Tissue Homeostasis, Injury, and Inflammation. *Immunity* 2015. **42**: 1005-1019.
- 2 **Liew, F. Y., Girard, J. P. and Turnquist, H. R.**, Interleukin-33 in health and disease. *Nat Rev Immunol* 2016. **16**: 676-689.
- 3 **Cayrol, C. and Girard, J. P.**, Interleukin-33 (IL-33): A nuclear cytokine from the IL-1 family. *Immunol Rev* 2018. **281**: 154-168.
- 4 **Bonilla, W. V., Frohlich, A., Senn, K., Kallert, S., Fernandez, M., Johnson, S., Kreutzfeldt, M., Hegazy, A. N., Schrick, C., Fallon, P. G., Klemenz, R., Nakae, S., Adler, H., Merkler, D., Lohning, M. and Pinschewer, D. D.**, The alarmin interleukin-33 drives protective antiviral CD8(+) T cell responses. *Science* 2012. **335**: 984-989.
- 5 **Baumann, C., Bonilla, W. V., Frohlich, A., Helmstetter, C., Peine, M., Hegazy, A. N., Pinschewer, D. D. and Lohning, M.**, T-bet- and STAT4-dependent IL-33 receptor expression directly promotes antiviral Th1 cell responses. *Proc Natl Acad Sci U S A* 2015. **112**: 4056-4061.

- 6 **Moussion, C., Ortega, N. and Girard, J. P.**, The IL-1-like cytokine IL-33 is constitutively expressed in the nucleus of endothelial cells and epithelial cells in vivo: a novel 'alarmin'? *PLoS One* 2008. **3**: e3331.
- 7 **Pichery, M., Mirey, E., Mercier, P., Lefrancais, E., Dujardin, A., Ortega, N. and Girard, J. P.**, Endogenous IL-33 is highly expressed in mouse epithelial barrier tissues, lymphoid organs, brain, embryos, and inflamed tissues: in situ analysis using a novel IL-33-LacZ gene trap reporter strain. *J Immunol* 2012. **188**: 3488-3495.
- 8 **Malhotra, D., Fletcher, A. L., Astarita, J., Lukacs-Kornek, V., Tayalia, P., Gonzalez, S. F., Elpek, K. G., Chang, S. K., Knoblich, K., Hemler, M. E., Brenner, M. B., Carroll, M. C., Mooney, D. J., Turley, S. J. and Immunological Genome Project, C.**, Transcriptional profiling of stroma from inflamed and resting lymph nodes defines immunological hallmarks. *Nat Immunol* 2012. **13**: 499-510.
- 9 **Carriere, V., Roussel, L., Ortega, N., Lacorre, D.-A., Americh, L., Aguilar, L., Bouche, G. and Girard, J.-P.**, IL-33, the IL-1-like cytokine ligand for ST2 receptor, is a chromatin-associated nuclear factor *in vivo*. *Proceedings of the National Academy of Sciences* 2007. **104**: 282-287.
- 10 **Choi, Y. S., Park, J. A., Kim, J., Rho, S. S., Park, H., Kim, Y. M. and Kwon, Y. G.**, Nuclear IL-33 is a transcriptional regulator of NF-kappaB p65 and induces endothelial cell activation. *Biochem Biophys Res Commun* 2012. **421**: 305-311.
- 11 **Ni, Y., Tao, L., Chen, C., Song, H., Li, Z., Gao, Y., Nie, J., Piccioni, M., Shi, G. and Li, B.**, The Deubiquitinase USP17 Regulates the Stability and Nuclear Function of IL-33. *Int J Mol Sci* 2015. **16**: 27956-27966.

- 12 **Lee, E. J., So, M. W., Hong, S., Kim, Y. G., Yoo, B. and Lee, C. K.**, Interleukin-33 acts as a transcriptional repressor and extracellular cytokine in fibroblast-like synoviocytes in patients with rheumatoid arthritis. *Cytokine* 2016. **77**: 35-43.
- 13 **Roussel, L., Erard, M., Cayrol, C. and Girard, J. P.**, Molecular mimicry between IL-33 and KSHV for attachment to chromatin through the H2A–H2B acidic pocket. *EMBO reports* 2008. **9**: 1006-1012.
- 14 **Gautier, V., Cayrol, C., Farache, D., Roga, S., Monsarrat, B., Burlet-Schiltz, O., Gonzalez de Peredo, A. and Girard, J. P.**, Extracellular IL-33 cytokine, but not endogenous nuclear IL-33, regulates protein expression in endothelial cells. *Sci Rep* 2016. **6**: 34255.
- 15 **Travers, J., Rochman, M., Miracle, C. E., Habel, J. E., Brusilovsky, M., Caldwell, J. M., Rymer, J. K. and Rothenberg, M. E.**, Chromatin regulates IL-33 release and extracellular cytokine activity. *Nat Commun* 2018. **9**: 3244.
- 16 **Stier, M. T., Mitra, R., Nyhoff, L. E., Goleniewska, K., Zhang, J., Puccetti, M. V., Casanova, H. C., Seegmiller, A. C., Newcomb, D. C., Kendall, P. L., Eischen, C. M. and Peebles, R. S., Jr.**, IL-33 Is a Cell-Intrinsic Regulator of Fitness during Early B Cell Development. *J Immunol* 2019. **203**: 1457-1467.
- 17 **Chang, J. E. and Turley, S. J.**, Stromal infrastructure of the lymph node and coordination of immunity. *Trends Immunol* 2015. **36**: 30-39.
- 18 **Rodda, L. B., Lu, E., Bennett, M. L., Sokol, C. L., Wang, X., Luther, S. A., Barres, B. A., Luster, A. D., Ye, C. J. and Cyster, J. G.**, Single-Cell RNA Sequencing of Lymph Node Stromal Cells Reveals Niche-Associated Heterogeneity. *Immunity* 2018. **48**: 1014-1028 e1016.

- 19 **Perez-Shibayama, C., Gil-Cruz, C. and Ludewig, B.**, Fibroblastic reticular cells at the nexus of innate and adaptive immune responses. *Immunol Rev* 2019. **289**: 31-41.
- 20 **Cyster, J. G., Ansel, K. M., Reif, K., Ekland, E. H., Hyman, P. L., Tang, H. L., Luther, S. A. and Ngo, V. N.**, Follicular stromal cells and lymphocyte homing to follicles. *Immunol Rev* 2000. **176**: 181-193.
- 21 **Huang, H.-Y., Rivas-Caicedo, A., Renevey, F., Cannelle, H., Peranzoni, E., Scarpellino, L., Hardie, D. L., Pommier, A., Schaeuble, K., Favre, S., Vogt, T. K., Arenzana-Seisdedos, F., Schneider, P., Buckley, C. D., Donnadieu, E. and Luther, S. A.**, Identification of a new subset of lymph node stromal cells involved in regulating plasma cell homeostasis. *Proceedings of the National Academy of Sciences* 2018. **115**: E6826-E6835.
- 22 **Luther, S. A., Tang, H. L., Hyman, P. L., Farr, A. G. and Cyster, J. G.**, Coexpression of the chemokines ELC and SLC by T zone stromal cells and deletion of the ELC gene in the plt:plt mouse. *Proc Natl Acad Sci U S A* 2000. **97**: 12694-12699.
- 23 **Link, A., Vogt, T. K., Favre, S., Britschgi, M. R., Acha-Orbea, H., Hinz, B., Cyster, J. G. and Luther, S. A.**, Fibroblastic reticular cells in lymph nodes regulate the homeostasis of naive T cells. *Nat Immunol* 2007. **8**: 1255-1265.
- 24 **Kallert, S. M., Darbre, S., Bonilla, W. V., Kreutzfeldt, M., Page, N., Muller, P., Kreuzaler, M., Lu, M., Favre, S., Kreppel, F., Lohning, M., Luther, S. A., Zippelius, A., Merkler, D. and Pinschewer, D. D.**, Replicating viral vector platform exploits alarmin signals for potent CD8(+) T cell-mediated tumour immunotherapy. *Nat Commun* 2017. **8**: 15327.

- 25 **Oboki, K., Ohno, T., Kajiwara, N., Arae, K., Morita, H., Ishii, A., Nambu, A., Abe, T., Kiyonari, H., Matsumoto, K., Sudo, K., Okumura, K., Saito, H. and Nakae, S.,** IL-33 is a crucial amplifier of innate rather than acquired immunity. *Proc Natl Acad Sci U S A* 2010. **107**: 18581-18586.
- 26 **Baekkevold, E. S., Roussigné, M., Yamanaka, T., Johansen, F.-E., Jahnsen, F. L., Amalric, F., Brandtzaeg, P., Erard, M., Haraldsen, G. and Girard, J.-P.,** Molecular Characterization of NF-HEV, a Nuclear Factor Preferentially Expressed in Human High Endothelial Venules. *The American Journal of Pathology* 2003. **163**: 69-79.
- 27 **Wherry, E. J., Blattman, J. N., Murali-Krishna, K., van der Most, R. and Ahmed, R.,** Viral Persistence Alters CD8 T-Cell Immunodominance and Tissue Distribution and Results in Distinct Stages of Functional Impairment. *Journal of Virology* 2003. **77**: 4911-4927.
- 28 **Wherry, E. J., Ha, S. J., Kaech, S. M., Haining, W. N., Sarkar, S., Kalia, V., Subramaniam, S., Blattman, J. N., Barber, D. L. and Ahmed, R.,** Molecular signature of CD8<sup>+</sup> T cell exhaustion during chronic viral infection. *Immunity* 2007. **27**: 670-684.
- 29 **Yang, C. Y., Vogt, T. K., Favre, S., Scarpellino, L., Huang, H. Y., Tacchini-Cottier, F. and Luther, S. A.,** Trapping of naive lymphocytes triggers rapid growth and remodeling of the fibroblast network in reactive murine lymph nodes. *Proc Natl Acad Sci U S A* 2014. **111**: E109-118.
- 30 **Chyou, S., Benahmed, F., Chen, J., Kumar, V., Tian, S., Lipp, M. and Lu, T. T.,** Coordinated regulation of lymph node vascular-stromal growth first by CD11c<sup>+</sup> cells and then by T and B cells. *J Immunol* 2011. **187**: 5558-5567.

- 31 **Gregory, J. L., Walter, A., Alexandre, Y. O., Hor, J. L., Liu, R., Ma, J. Z., Devi, S., Tokuda, N., Owada, Y., Mackay, L. K., Smyth, G. K., Heath, W. R. and Mueller, S. N.,** Infection Programs Sustained Lymphoid Stromal Cell Responses and Shapes Lymph Node Remodeling upon Secondary Challenge. *Cell Rep* 2017. **18:** 406-418.
- 32 **Scandella, E., Bolinger, B., Lattmann, E., Miller, S., Favre, S., Littman, D. R., Finke, D., Luther, S. A., Junt, T. and Ludewig, B.,** Restoration of lymphoid organ integrity through the interaction of lymphoid tissue-inducer cells with stroma of the T cell zone. *Nat Immunol* 2008. **9:** 667-675.
- 33 **Mueller, S. N., Hosiawa-Meagher, K. A., Konieczny, B. T., Sullivan, B. M., Bachmann, M. F., Locksley, R. M., Ahmed, R. and Matloubian, M.,** Regulation of homeostatic chemokine expression and cell trafficking during immune responses. *Science* 2007. **317:** 670-674.
- 34 **Mueller, S. N., Matloubian, M., Clemens, D. M., Sharpe, A. H., Freeman, G. J., Gangappa, S., Larsen, C. P. and Ahmed, R.,** Viral targeting of fibroblastic reticular cells contributes to immunosuppression and persistence during chronic infection. *Proc Natl Acad Sci U S A* 2007. **104:** 15430-15435.
- 35 **Chai, Q., Onder, L., Scandella, E., Gil-Cruz, C., Perez-Shibayama, C., Cupovic, J., Danuser, R., Sparwasser, T., Luther, S. A., Thiel, V., Rulicke, T., Stein, J. V., Hehlhans, T. and Ludewig, B.,** Maturation of lymph node fibroblastic reticular cells from myofibroblastic precursors is critical for antiviral immunity. *Immunity* 2013. **38:** 1013-1024.
- 36 **Schaeuble, K., Cannelle, H., Favre, S., Huang, H. Y., Oberle, S. G., Speiser, D. E., Zehn, D. and Luther, S. A.,** Attenuation of chronic antiviral T-cell responses

through constitutive COX2-dependent prostanoid synthesis by lymph node fibroblasts. *PLoS Biol* 2019. **17**: e3000072.

37 **Bessa, J., Meyer, C. A., de Vera Mudry, M. C., Schlicht, S., Smith, S. H., Iglesias, A. and Cote-Sierra, J.**, Altered subcellular localization of IL-33 leads to non-resolving lethal inflammation. *J Autoimmun* 2014. **55**: 33-41.

38 **Mempel T.R, H. S. E., von Andrian U.H.**, T-cell priming by dendritic cells in lymph nodes occurs in three distinct phases. *Nature* 2004. **427**: 154-158.

39 **Bajenoff, M., Egen, J. G., Koo, L. Y., Laugier, J. P., Brau, F., Gleichenhau, N. and Germain, R. N.**, Stromal cell networks regulate lymphocyte entry, migration, and territoriality in lymph nodes. *Immunity* 2006. **25**: 989-1001.

40 **Shlomovitz, I., Erlich, Z., Speir, M., Zargarian, S., Baram, N., Engler, M., Edry-Botzer, L., Munitz, A., Croker, B. A. and Gerlic, M.**, Necroptosis directly induces the release of full-length biologically active IL-33 in vitro and in an inflammatory disease model. *FEBS J* 2019. **286**: 507-522.

41 **Kakkar, R., Hei, H., Dobner, S. and Lee, R. T.**, Interleukin 33 as a mechanically responsive cytokine secreted by living cells. *J Biol Chem* 2012. **287**: 6941-6948.

42 **Kearley, J., Silver, J. S., Sanden, C., Liu, Z., Berlin, A. A., White, N., Mori, M., Pham, T. H., Ward, C. K., Criner, G. J., Marchetti, N., Mustelin, T., Erjefalt, J. S., Kolbeck, R. and Humbles, A. A.**, Cigarette smoke silences innate lymphoid cell function and facilitates an exacerbated type I interleukin-33-dependent response to infection. *Immunity* 2015. **42**: 566-579.

- 43 **Chen, W. Y., Hong, J., Gannon, J., Kakkar, R. and Lee, R. T.**, Myocardial pressure overload induces systemic inflammation through endothelial cell IL-33. *Proc Natl Acad Sci U S A* 2015. **112**: 7249-7254.
- 44 **Bazigou, E., Lyons, O. T., Smith, A., Venn, G. E., Cope, C., Brown, N. A. and Makinen, T.**, Genes regulating lymphangiogenesis control venous valve formation and maintenance in mice. *J Clin Invest* 2011. **121**: 2984-2992.
- 45 **Patro, R., Duggal, G., Love, M. I., Irizarry, R. A. and Kingsford, C.**, Salmon provides fast and bias-aware quantification of transcript expression. *Nat Methods* 2017. **14**: 417-419.
- 46 **Soneson, C., Love, M. I. and Robinson, M. D.**, Differential analyses for RNA-seq: transcript-level estimates improve gene-level inferences. *F1000Res* 2015. **4**: 1521.
- 47 **Law, C. W., Chen, Y., Shi, W. and Smyth, G. K.**, voom: Precision weights unlock linear model analysis tools for RNA-seq read counts. *Genome Biol* 2014. **15**: R29.
- 48 **Battegay, M., Cooper, S., Althage, A., Banziger, J., Hengartner, H. and Zinkernagel, R. M.**, Quantification of lymphocytic choriomeningitis virus with an immunological focus assay in 24- or 96-well plates. *J Virol Methods* 1991. **33**: 191-198.